







Liquid crystal doped photopolymer micro-droplets printed by a simple and clean laser-induced forward transfer process

DANIEL PUERTO,^{1,2,*}  SERGI GALLEGU,^{1,2}  CATALIN CONSTANTINESCU,³ CAMILO FLORIAN,⁴  MANUEL ORTUÑO,^{1,2} ANDRÉS MÁRQUEZ,^{1,2}  JORGE FRANCÉS,^{1,2} INMACULADA PASCUAL,^{2,5}  AUGUSTO BELENDEZ,^{1,2}  AND PATRICIA ALLONCLE³

¹*Dept. Física, Enginyeria de Sistemes i Teoria del Senyal, Universitat d'Alacant, 03690, San Vicente del Raspeig, Spain*

²*I.U. Física Aplicada a Ciencias y Tecnologías, University of Alicante, 03690, San Vicente del Raspeig, Spain*

³*Aix-Marseille University, CNRS, UMR 7341 LP3, 13009, Marseille, France*

⁴*Princeton Institute for the Science and Technology of Materials, Princeton University, Princeton, NJ 08544, USA*

⁵*Dept. Óptica, Farmacologia i Anatomia, Universitat d'Alacant, 03690, San Vicente del Raspeig, Spain*

**dan.puerto@ua.es*

Abstract: We print a tunable photopolymer (photopolymer dispersed liquid crystal -PDLC), using the laser-induced direct transfer technique without absorber layer, which was a challenge for this technique given the low absorption and high viscosity of PDLC, and which had not been achieved so far to our knowledge. This makes the LIFT printing process faster and cleaner and achieves a high-quality printed droplet (aspheric profile and low roughness). A femtosecond laser was needed to reach sufficiently peak energies to induce nonlinear absorption and eject the polymer onto a substrate. Only a narrow energy window allows the material to be ejected without spattering.

© 2023 Optica Publishing Group under the terms of the [Optica Open Access Publishing Agreement](#)

1. Introduction

The constant development of the small and compact vision systems for use in areas such as medicine, security or digital devices also implies the development of the elements that compose them. In this respect, the manufacturing of miniaturized optical elements such as waveguides or lenses is posing a challenge [1,2]. Initially, planar processing techniques such as sol-gel [3,4] or photolithography [5,6], which requires expensive instrumentation, were used. In the case of lens, to fabricate lens arrays for high field-of-view (FOV) devices, complex techniques are needed that allow precise alignment of the lens with the rest of the optical system and be manufactured on flexible surfaces. This was achieved with the reconfigurable soft lithography technique [7,8] that uses elastomeric polymers such as polydimethylsiloxane (PDMS) as a mask. Nevertheless, the low quality of lens arrays created by using PDMS membranes with a poorly controllable profile, low fill factor (FF = 30-90%) and macroscopic size, led to the search for alternative techniques such as multiphoton polymerization [9] suitable for the fabrication of three-dimensional and arbitrary designed microstructures. The manufacturing time with this technique is considerably longer than the previous ones (tens of hours), which limits the size of the lens arrays that can be manufactured. For this reason, Wu et al. [10] proposed high-speed voxel (pixel) modulation laser scanning technique (HVLS) that reduces the matrix manufacturing process to a few hours yet without losing surface texture quality.

The long manufacturing time, typical for these multistep techniques, is incompatible with mass production processes. In this sense, a two-step manufacturing method based on droplets deposition by laser-induced forward transfer (LIFT), which had previously been used for printing polymers [11], and the UV exposure to cross-link the droplets was proposed that reduces manufacturing time while maintaining a good quality of the planoconvex microlenses [12]. LIFT has also been used to fabricate titanium-in-diffused lithium niobate waveguide mode filters [13], opening the use of this direct laser writing technique in the fabrication of photonic devices. Although recent advances in inkjet printing technology have made it possible to print a wide variety of polymeric devices with a high degree of control over the print position [14,15], LIFT, unlike inkjet printing [16,17], can be used with photopolymers with viscosities even higher than 50 mPa s [18] and allows better control over print position and smaller droplet size [11]. However, full control of the droplet geometry is still not achieved following this technique, being limited to circular profiles, which does not allow a precise control of the fill factor (FF) in the case of lens arrays. Therefore, Duocastella et al. [19] proposed an evolution of the LIFT technique, called Laser Catapulting (LCP), which transfers solid polymeric microdisks in the first step and then through a thermal reflux process converts the microdisks into microdroplets. They achieve to produce arrays of circular, triangular, and cylindrical microdroplets with a radius between 50–250 μm and 100% fill-factor [20].

The main problem with both techniques is the low laser absorption and high viscosity of the polymers used for the fabrication of flexible photonic devices, which makes their transfer difficult and therefore limits the type of materials to be used. To overcome this limitation, a thin layer (few nanometers) of absorbent material (e.g. titanium), which is called dynamic release layer (DRL) or sacrificial layer [21], is usually used [22]. This layer absorbs the energy of the laser, and in its expulsion process, it propels the deposited material (polymer) on it, favouring its transfer. The main disadvantage of metallic DRLs is related to contamination of the transferred material with removed DRL metallic particles, as these can affect the performance of printed devices. This effect can be mitigated by using a thin layer of highly absorbent polymer like DRL, which is known as Blister-Actuated Laser-Induced Forward Transfer (BA-LIFT) [23]. In addition, this polymer DRL absorbs a large part of the laser energy, preventing damage to the material to be printed. The transfer mechanism is based on the formation of a rapidly expanding blister that deforms plastically, propelling the material to transfer, which continues to move toward the receiving substrate. Below critical laser energy, the blister remains sealed, preventing contamination with DRL ablation particles in the transfer process. However, in many cases, it is necessary to overcome this critical energy in order to transfer the donor polymer due to its high viscosity or a greater thickness of the donor layer. In these cases, some DRL ablation particles can contaminate the printed devices.

The low absorption of polymers has led to the use of femtosecond laser pulses to induce multiphoton absorption of the material and to eject the polymer in LIFT printing [11]. However, as Banks et al. show [24], printing without DRL has poor quality because it does not print the entire pixel. Another more successful attempt with femtosecond laser and without DRL layer was made by Duocastella et al. [25], who managed to print water and glycerol 20% (v/v) droplets. For this they had to focus the laser with a beam waist at the focus of about 1.2 μm , taking advantage of the self-focusing of the beam inside the liquid. In this way they manage to generate a plasma inside the low absorber liquid that induces the formation of the cavitation bubble. However, the printing process of this technique, known as film-free laser forward printing, depends on the focus depth [26], since micrometre variations in this induces changes of the same order in the diameter of the droplet. Therefore, this technique is not compatible with the mass production of optical elements of the same characteristics and properties.

In this work, we demonstrate how it is possible to print a low laser absorption and high viscosity tunable polymer (PDLC, photopolymer dispersed liquid crystal [27]) by using the LIFT technique,

without metallic or polymeric DRL, in a simpler and cleaner direct transfer process. We achieve this goal by controlling the printing parameters such as laser energy, pulse duration, or donor layer thickness. In this way, we fabricate microdroplets and characterize their morphology. The use of a dynamic liquid crystal photopolymer opens the door to creating tunable micro-devices.

2. Material and methods

LIFT system (Fig. 1(a)) has been performed with a femtosecond laser (CARBIDE, LIGHT CONVERSION; wavelength = 1030 nm; pulse duration 190 fs – 20 ps; max. repetition rate = single shot to 2 MHz; maximum output pulse energy of 2 mJ). A wave plate and a polarizing beam-splitter cube control the pulse energy (Figure 1(a)). The laser beam is scanned by a galvanometric mirror (SCANLAB laserDESK) and focused by an F-theta telecentric objective (LINOS F-Theta-Ronar telecentric, focal length = 70 mm, $\lambda = 1030 - 1080$ nm). The diameter of the Gaussian beam is $\sim 50 \mu\text{m}$ (at $1/e^2$), obtained with a representation of the diameter of the ablation crater as a function of the natural logarithm of the laser pulse energy, proposed by Liu et al. [28]. However, preliminary tests with DRL layer have been carried out by using a Léopard (Continuum) laser system with a pulse duration of 50 ps, 10 Hz and a wavelength of 1064 nm. In both systems, a camera is used to have a precise control of the distances between the donor and the substrate, which is called gap. After the printing process a light-curing of the polymer droplets are made using an ultra-intense white light lamp, allowing the process to be carried out with only 2 minutes of irradiation.

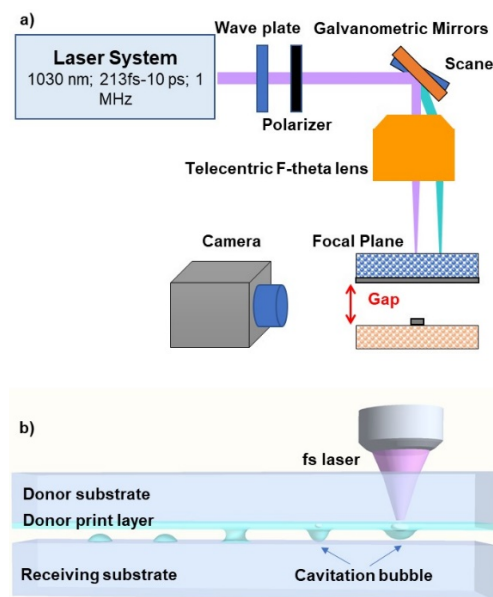


Fig. 1. a) Schematic of the experimental system used in polymer printing. It includes a laser with a variable pulse duration between 210 fs and 10 ps, a wavelength of 1030 nm and a repetition frequency of up to 1 MHz. In addition, it includes a scanner and an F-theta lens that allows you to move the position of the focus of the laser along a $5 \times 5 \text{ cm}^2$ surface. b) Schematic of the printing process.

The donor consisted of a glass slide with a thin ($\sim \mu\text{m}$) photopolymer layer (PDLC). The PDLC is composed of the nematic liquid crystal (Licristal BL036) purchased from Merck, and dipentaerythritol penta-/hexaacrylate (DPHPA) with a refractive index $n = 1.490$ as monomer. N-Vinyl-2-pyrrolidone was used as crosslinker (NVP), N-phenyl glycine (NPG) as radical

generator, and octanoic acid (OA) as cosolvent [24,29]. We used ethyl eosin (Yet) as dye due to the wide experience of our research team in hydrophilic photopolymers with yellowish eosin [30]. N-Methyl-2-pyrrolidone acts as a solvent in this formulation, allowing the dye to dissolve easily, and is also used in combination with NVP to control the overmodulation during the photopolymerization process. Furthermore, it allows to reduce the viscosity of the formulation, since NMP has a low viscosity in relation to the monomer. This material is tunable by applying a voltage, even after the photopolymerization [31]. The PDLC has a measured viscosity of 600 mPa s (Anton Paar modular compact rheometer, model MCR 102), not only well above the limit for regular inkjet printing [15], but also higher than most other polymers that have been previously used to print droplets [11,21,22].

The topography of micro-droplets has been measured with an interferometric confocal microscope (model DCM3D from Leica, objectives 5x, 20x, 50x, 150x) and an atomic force microscope (Advanced Scanning Probe Microscope, model XE-100, from Park Systems).

The glass slide is treated on the surface by a plasma torch to achieve better adherence and homogeneous surface coverage. The homogeneous PDLC layer was created by using a simple spin coating system. A parametric study carried out to determine the optimal thickness of the polymer layer in such a way that it was thin enough to be expelled with the laser and, in turn, thick enough so that the ejection was stable and generated the droplets. Due to the small window of optimal results (maximum two energies for each layer thickness), we do not show these results. However, ensuing this parametric study, a thickness of around 4 μm was found to be optimal, with spin coater (Laurel Technologies Corporation, model WS-400A-8NPP/LITE) deposition parameters of 3000 revolutions per minute (RPM), ramp of 500 RPM per second, and 30 seconds of continuous spinning.

We used two types of substrates; on the one hand we used glass slides for the first tests and to find the optimal printing parameters. This glass produces a contact angle of 26.5° with PDLC, statistically measured in the laboratory. The second type of substrate is a glass slide coated with a thin layer (25 nm) of indium tin oxide (ITO, resistance of $80 \sim 100 \Omega/\text{sq}$ and transmittance $> 87\%$), that induces a contact angle of 22.5° , statistically measured. This type of substrate will receive the propelled polymer and will be used to induce an electric field in the PDLC liquid crystal molecules and modify the optical properties of photonic devices fabricated with this material.

3. Results and discussion

Given that this is the first time PDLC has been printed, that it has high viscosity (600 mPa.s) and low absorption at the wavelengths of the lasers used in the study (IR), and that the literature shows that, in general, even with ultraviolet lasers [32,33] or ultrashort pulses (femtosecond [11,21]) a DRL layer is used to print low absorption polymers by LIFT, we started the study by employing a thin DRL layer to try to print PDLC. Therefore, we deposited a thin DRL of highly absorbent titanium (50 nm) on the slide, which absorb the laser energy (50 ps; 1064 nm) and volatilizes, inducing the ejection of the PDLC, as shown in figure 2(a). At high energies, i.e. 400–1100 μJ , the ejected material generates splashes around the main droplet which does not have a circular profile. However, as we reduce the energy, the spattering disappears, the droplet takes on a more circular profile and with a smaller radius. At 95 μJ , we observe that not all irradiations generate the ejection of a polymer droplet, this value being the energy limit (threshold) for printing this material.

Generally, LIFT printing of liquid materials process occurs after the formation of a cavitation bubble that collapses, forming a jet of fluid that, after breaking away from the donor, reaches the substrate located at a certain distance (gap) [34,35]. In the case of materials with high viscosity and plasticity, the printing process can be carried out without breakup the jet from the donor layer [36] (Fig. 1(b)). In these cases, the distance between the donor and the substrate is critical



Fig. 2. Images of the photopolymer droplets deposited on the substrate with a picosecond laser: a) at different laser energies and a distance (gap) between donor and substrate of 50 μm ; b) at different distance (gap) between donor and substrate and an energy of 215 μJ . All the images were obtained with an optical microscope by using a 5x objective and are sharing the same scale bar.

(gap), since, as shown in [11], for very small distances the expelled material adheres to the substrate without separating from the donor and both remain attached indefinitely. On the other hand, when the distance is very large, an intense splashing process is observed. Only a small gap distance range allows the printing of a clean droplet, probably created by the contact of the cavitation bubble with the substrate, since the bubble size is of the order of these gaps. Studying this parameter (Fig. 2(b)), we found that between 20 and 100 μm we were able to print with an adequate droplet size and profile for an energy of 215 μJ without splashing process, a sufficiently wide range that does not make this parameter so critical.

The quality (aspheric profile, surface roughness, etc.) of these droplets can be observed in the microscope image in figure 3.a, i.e. droplets have a circular profile, $\sim 80 \mu\text{m}$ of diameter. It is important to note that in the upper area of the lens there are some titanium microparticles that were deposited as an effect of the titanium ejection process. These particles affect the optical performance and quality of the droplets. By using a confocal microscope, we measured the three-dimensional profile of the droplets before (Fig. 3(b)) and after (Fig. 3(c)) the light-curing process.

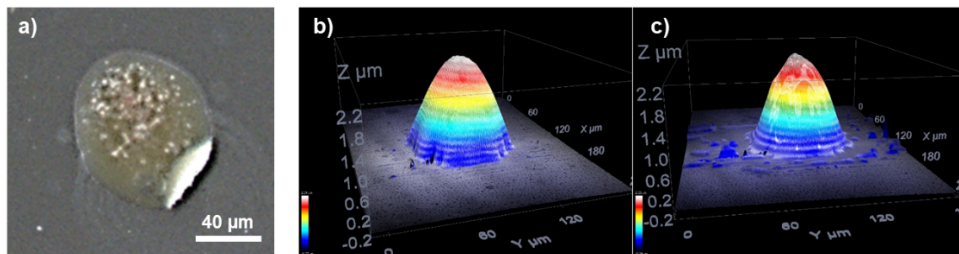


Fig. 3. a) Microscope image of the photopolymer droplet deposited with a picosecond laser at an energy of 215 μJ and a gap of 70 μm . 3D topographic profile of a printed photopolymer droplet by using a distance (gap) between donor and recipient of 50 μm and a picosecond laser energy of 115 μJ , before b) and after c) the photopolymerization process, taken with a confocal microscope by using a 50x objective.

As it can be seen, the diameter of this droplet is $\sim 80 \mu\text{m}$, while its height is 2.2 μm . Because titanium is highly absorbent when we illuminate the material with a powerful white light source to induce its photopolymerization, it has a temperature increasing effect that melts this material, as we see in the upper part of the droplet in figure 3(c), but also evaporates part of the polymer. This worsens the profile of the droplet, and also affects its optical quality. Therefore, one of the challenges is to print polymer droplets without the need for a thin absorption layer.

To address the challenge of printing without using a DRL layer, we first tested the feasibility of printing PDLC using two different picosecond infrared lasers (pulse duration of 10 and 50 ps) and found that the material cannot be transferred at these pulse durations without using a DRL layer, as the material does not absorb enough energy. Therefore, the laser pulse duration was

reduced to the femtosecond range (213 fs) to increase the peak power and favour the non-linear absorption of the photons by the material. Preserving the previously obtained donor-substrate distance conditions (75 μm), in figure 4 we study the printing at different energies (2.25–1 μJ). These energies are below the ablation threshold of the glass slides, avoiding their deterioration, which have been verified after the irradiation processes. Different droplets are shown for each energy to demonstrate the repeatability of the process. The most remarkable fact is that we were able to print a low absorbing polymer such as PDLC by using femtosecond laser pulses at lower energies than those used with the picosecond laser and DRL-layer, showing the effectiveness of multiphoton absorption at this pulse duration. At high energies ($>2 \mu\text{J}$) a spattering process occurs at each irradiation, which fouls the area without forming a specific single droplet. For energy values between 1.9 and 1.6 μJ , this spattering is reduced and only a single polymer droplet is printed. Only at 1.5 μJ there is a clean surface observed with a single droplet. For energy values below 1.5 μJ , no material is ejected. We also note the different size of the droplets. While the droplets generated with 1.5 μJ have a size of 10 μm , those produced with 1.66 μJ have a size of 25 μm and those with 1.88 μJ have a size of 33 μm , which are smaller than those generated with picosecond laser and DRL layer (80 μm , Fig. 3). The small black dots in the 1.66 μJ and 1.5 μJ images are defects on the glass surface.

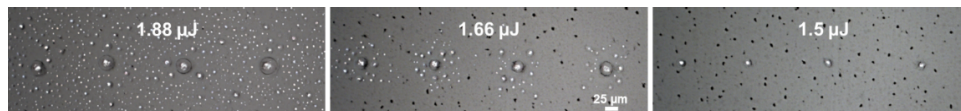


Fig. 4. Microscope image of the photopolymer droplet deposited on the substrate with a femtosecond laser at different laser energies and a gap of 75 μm . The images were obtained with an optical microscope using a 50x objective.

Since the laser spot size is the same for picosecond and femtosecond irradiations, the large difference in droplets size indicates that the absorption area of the laser energy is much smaller when we do not use the DRL layer with the femtosecond pulse, even though the peak power is almost double for this case (7 MW vs. 4.3 MW). The small window that allows the printing of droplets without spattering (1.42–1.58 μJ) is also associated with the small area of absorption of the laser energy. Since only the peak energy on the Gaussian profile, that corresponds to the highest energy region, can induce a cavitation bubble, the resulting bubble size will be quite small. This means that an increase of the pulse energy will noticeably increase the local temperature and the internal gas pressure inside the bubble, increasing the likelihood of liquid instabilities that result in violent bubble collapse, producing unwanted liquid splash. This small window of energies is also observed for irradiations that generate a droplet, without or with splashes in its surroundings, being more stable in the picosecond with DRL-layer case due to the larger size of the cavitation bubble.

Figure 5 shows the topographic profile of the droplets generated at 1.5 μJ obtained with a confocal microscope. Here, we can see that the diameter of the droplets is 10 μm , while the height of the droplets is about 300 nm, about eight times smaller than the droplet made with DRL layer. That means a volume three orders of magnitude smaller (15.7 fL) than drops printed with DRL layer (5.5 pL), which gives us an idea of the small cavitation bubble created and the minimal contact of the droplet with the substrate sample, which makes this printing process very complex compared to other more absorbent materials.

Having achieved the goal of printing a low-absorbent polymer without using a DRL layer, the next objective is to be able to print this polymer with liquid crystal on a conductive material that allows its use for the manufacture of tunable devices. A glass slide coated with a thin layer (25 nm) of indium tin oxide (ITO), which is both conductive and transparent in the visible spectrum, was used as the substrate. Therefore, the printing is done on the ITO layer. Since the

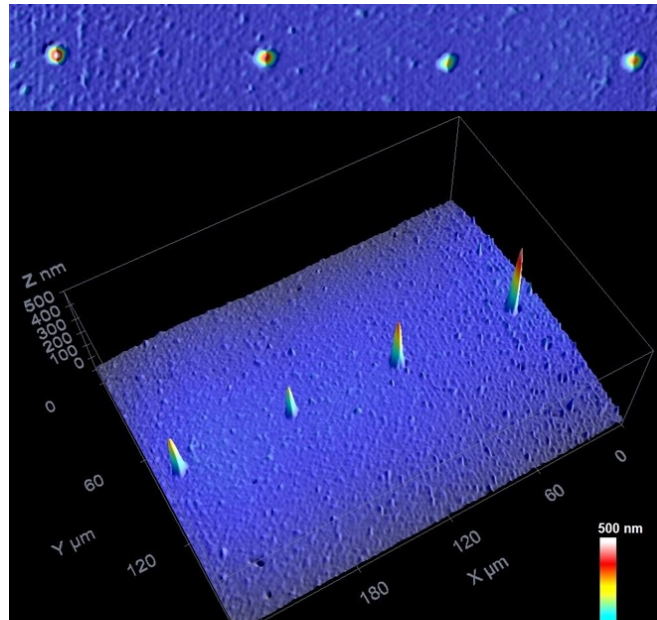


Fig. 5. 3D image of the polymer droplets deposited on a glass sample holder with a femtosecond laser under conditions of a 75 μm gap and an energy of 1.5 μJ obtained with a confocal microscope with a 50x objective.

contact angle (surface tension) of ITO and glass show a small difference, several tests had to be carried out to adjust the irradiation parameters to the ITO surface (Fig. 6). The figure 6(a) shows a printed droplet array with an energy of 1.5 μJ and a gap of 60 μm , demonstrating the reproducibility of the technique with a 98% success rate in printing drops with good quality profile and no spattering. It is found that the energy window for splash-free printing is the same as in the case of glass, i.e. printing is only possible with an energy around 1.5 μJ (Fig. 6(b)) and less energy it is not possible to print.

However, the effect of the small surface tension difference is observed with the range of gap values for which splash-free printing is possible (60 μm Fig. 6(b) and 75 μm 6c), where it is observed that for gap of 75 μm (Fig. 6(c)) or higher and an energy of 1.5 μJ it is not possible to print on the ITO surface. In these cases, since the jet of material is formed, as it collapses, a splashing process occurs as seen with the small droplets on the surface in Figure 6(c). Despite the small energy window and Gap, making the printing process even more difficult, the quality of the droplets is still good, as we can see in figure 6(b), presenting a better circular profile than that achieved with glass. Furthermore, it is interesting to note an additional modification induced on the surface of the ITO. It occurs when the laser beam that is not absorbed by the polymer in the printing process passes through the ITO surface, inducing its modification. This modification is a phase change as observed in previous investigations [37] and forms that dark circle surrounded by a curious ring of a reflection greater than that of the ITO itself. These phase changes induce small variations in material resistivity [38]. Since the confocal microscope measurement is based on an interference process, this phase shift on the surface of the ITO masks the actual measurement of the topography of the polymer droplets.

In order to measure the topography of the droplets on ITO and to validate the results obtained with the confocal microscope of the droplets printed on the glass, we have used an atomic force microscope (AFM, Fig. 6(d) and 6(e)). In these results we can observe that the drops deposited on the slide with ITO (Fig. 6(e)) have a more spherical profile than those deposited on glass

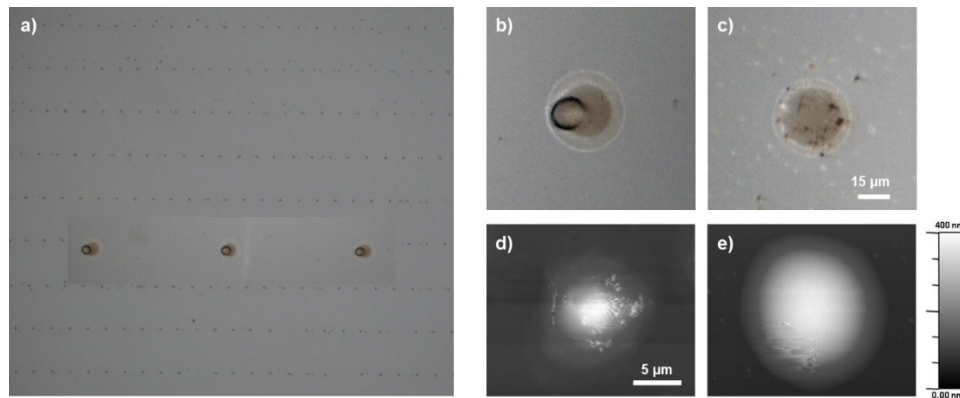


Fig. 6. Optical microscope images of droplets deposited on a glass slide with ITO generated with 1.5 μJ and a gap of 60 μm (a, array) and (b, single droplet) and 75 μm (c). The images were obtained with an optical microscope using a 100x objective. 3D image of the topographical profile of polymer droplets deposited with an energy of 1.5 μJ on a glass slide at a gap of 75 μm (d) and on an ITO at a gap of 60 μm (e) obtained with an atomic force microscope after solidification.

(Fig. 6(d)), which demonstrates the different adhesion behaviour of the polymer depending on the substrate surface (adhesion/surface tension), being more adherent on the ITO which has a lower contact angle (surface tension), which makes the optical properties of the droplets on ITO a priori better than those made on glass. Furthermore, it can be observed that the droplets on ITO have a larger diameter, 15 μm compared to 10 μm on glass, and a smaller height, 350 nm compared to 400 nm. This shows that the amount of material ejected is of the same order of magnitude in both cases, 15.7 fL in glass and 31 fL in ITO, although it is about twice as much in ITO, where the greater adhesion of the material to the surface allows for a more spherical profile. The interaction of forces between substrate adhesion and jet pulling force determine the amount of material deposited on the substrate [11]. Due to the droplet size ($\sim\mu\text{m}$) the effects of gravity on droplet formation (sphericity) are omitted. Therefore, the greater amount of material deposited on ITO confirms its greater adherence, just as its lower height confirms its smaller contact angle. In the same sense, although the contact angle in ITO is 22.5° and in glass is 26.5° , the contact angles of the droplets generated with LIFT are 2.7° and 4.6° respectively, being the double in glass, which shows its lower adherence, given that the force with which the polymer jet impacts on the substrate surface must be the same as in ITO, since both the laser energy and thickness are the same. The very low value of the contact angle of the droplets deposited by LIFT is due to the speed at which the droplets reach the surface, which causes the pressure to reduce their vertical size. This affects the aspect ratio between diameter and height, which is quite small, and is a challenge we must overcome in the near future if we want to create tunable lenses or waveguides with controllable aspect ratio.

4. Conclusion

In conclusion, we have succeeded for the first time in printing a low absorption and high viscosity liquid crystal doped photopolymer, such as PDLC, without using a DRL layer, which makes the printing process faster and cleaner. This required the use of a femtosecond laser, which made it possible to achieve sufficiently high peak energies to induce multiphoton absorption of the polymer and ejection onto a substrate. It has been found that the energy window that allows this ejection process without causing spattering around the main droplet is very small (around 1.5 μJ). Moreover, as already observed by other authors, it has been confirmed that given the

high density and plasticity of the polymer, only a cavitation bubble is formed and not a jet of material, so the distance between the donor and the substrate must be very small ($<100\ \mu\text{m}$). In this regard, we have also found that this distance is much more critical for the case of a substrate with ITO, where printing is achieved for distances of $60\ \mu\text{m}$ or less, indicating the importance of the surface properties of the material to achieve printing, as well as to control the volume of the printed material. Since PDLC is a tunable material with liquid crystal molecules, the ability to be printed on ITO is key for the fabrication of tunable devices, from lenses with variable focal lengths to optical switches.

Funding. European Research Council (“FOCUSIS” grant agreement 844977); Universidad de Alicante (ACIE-20-10, UTALENTO18-10); Ministerio de Ciencia e Innovación (PID2019-106601RB-I00, PID2021-123124OB-I00); Conselleria de Innovación, Universidades, Ciencia y Sociedad Digital, Generalitat Valenciana (BEST/2021/021, IDIFEDER/2021/014, PROMETEO/2021/006).

Disclosures. The authors declare no conflicts of interest.

Data availability. No data were generated or analyzed in the presented research.

References

1. H. P. Herzig, *Micro-Optics: Elements, Systems and Applications* (CRC Press, London, 2014).
2. R. He, C. Teng, S. Kumar, C. Marques, and R. Min, “Polymer Optical Fiber Liquid Level Sensor: A Review,” *IEEE Sensors J.* **22**(2), 1081–1091 (2022).
3. A. Bahtat, M. Bouderbala, M. Bahtat, M. Bouazaoui, J. Mugnier, and M. Druetta, “Structural characterisation of Er³⁺ doped sol-gel TiO₂ planar optical waveguides,” *Thin Solid Films* **323**(1-2), 59–62 (1998).
4. F.-H. Zhao, Y.-J. Xie, S.-P. He, S.-J. Fu, and Z.-W. Lu, “Single step fabrication of microlens arrays with hybrid HfO₂-SiO₂ sol-gel glass on conventional lens surface,” *Opt. Express* **13**(15), 5846–5852 (2005).
5. D. Radtke, J. Duparre, U. D. Zeitner, and A. Tunnermann, “Laser lithographic fabrication and characterization of a spherical artificial compound eye,” *Opt. Express* **15**(6), 3067–3077 (2007).
6. Y. Huang, Q. Zhao, L. Kamyab, A. Rostami, F. Capolino, and O. Boyraz, “Sub-micron silicon nitride waveguide fabrication using conventional optical lithography,” *Opt. Express* **23**(5), 6780–6786 (2015).
7. Y. Xia, E. Kim, XM Zhao, JA Rogers, M Prentiss, and GM Whitesides, “Complex Optical Surfaces Formed by Replica Molding Against Elastomeric Masters,” *Science* **273**(5273), 347–349 (1996).
8. L. P. Lee and R. Szema, “Inspirations from Biological Optics for Advanced Photonic Systems,” *Science* **310**(5751), 1148–1150 (2005).
9. R. Guo, S. Xiao, X. Zhai, J. Li, A. Xia, and W. Huang, “Micro lens fabrication by means of femtosecond two photon photopolymerization,” *Opt. Express* **14**(2), 810–816 (2006).
10. D. Wu, J.-N. Wang, L.-G. Niu, X. L. Zhang, S. Z. Wu, Q.-D. Chen, L. P. Lee, and H. B. Sun, “Bioinspired Fabrication of High-Quality 3D Artificial Compound Eyes by Voxel-Modulation Femtosecond Laser Writing for Distortion-Free Wide-Field-of-View Imaging,” *Adv. Opt. Mater.* **2**(8), 751–758 (2014).
11. B. Thomas, A.P. Alloncle, P. Delaporte, M. Sentis, S. Sanaur, M. Barret, and P. Collot, “Experimental investigations of laser-induced forward transfer process of organic thin films,” *Appl. Surf. Sci.* **254**(4), 1206–1210 (2007).
12. C. Florian, S. Piazza, A. Diaspro, P. Serra, and M. Duocastella, “Direct Laser Printing of Tailored Polymeric Microlenses,” *ACS Appl. Mater. Interfaces* **8**(27), 17028–17032 (2016).
13. K. S. Kaur, A. Z. Subramanian, Y. J. Ying, D. P. Banks, M. Feinaeugle, P. Horak, V. Apostolopoulos, C. L. Sones, S. Mailis, and R. W. Eason, “Waveguide mode filters fabricated using laser-induced forward transfer,” *Opt. Express* **19**(10), 9814–9819 (2011).
14. M. Nadgorny and A. Ameli, “Functional Polymers and Nanocomposites for 3D Printing of Smart Structures and Devices,” *ACS Appl. Mater. Interfaces* **10**(21), 17489–17507 (2018).
15. E. V. Blynskaya, S. V. Tishkov, K. V. Alekseev, A. A. Vetcher, A. I. Marakhova, and D. T. Rejepov, “Polymers in Technologies of Additive and Inkjet Printing of Dosage Formulations,” *Polymers* **14**(13), 2543 (2022).
16. B.-J. de Gans, P. C. Duineveld, and U. S. Schubert, “Inkjet Printing of Polymers: State of the Art and Future Developments,” *Adv. Mater.* **16**(3), 203–213 (2004).
17. D. Jang, D. Kim, and J. Moon, “Influence of Fluid Physical Properties on Ink-Jet Printability,” *Langmuir* **25**(5), 2629–2635 (2009).
18. K. Hölzl, S. Lin, L. Tytgat, S. V. Vlierberghe, L. Gu, and A. Ovsianikov, “Influence of Fluid Physical Properties on Ink-Jet Printability,” *Biofabrication* **8**(3), 032002 (2016).
19. S. Surdo, R. Carzino, A. Diaspro, and M. Duocastella, “Single-Shot Laser Additive Manufacturing of High Fill-Factor Microlens Arrays,” *Adv. Opt. Mater.* **6**(5), 1701190 (2018).
20. S. Surdo, A. Diaspro, and M. Duocastella, “Geometry-controllable micro-optics with laser catapulting,” *Opt. Mater. Express* **9**(7), 2893–2901 (2019).
21. W.A. Tolbert, I.-Y.S. Lee, M.M. Doxtader, E.W. Ellis, and D.D. Dlott, “High-speed color imaging by laser ablation transfer with a dynamic release layer: Fundamental mechanisms,” *J. Imaging Sci. Technol.* **37**(4), 411–421 (1993).

22. L. Rapp, C. Cibert, A.P. Alloncle, and P. Delaporte, "Characterization of organic material micro-structures transferred by laser in nanosecond and picosecond regimes," *Appl. Surf. Sci.* **255**(10), 5439–5443 (2009).
23. N.T. Kattamis, P.E. Purnick, R. Weiss, and C.B. Arnold, "Thick film laser induced forward transfer for deposition of thermally and mechanically sensitive materials," *Appl. Phys. Lett.* **91**(17), 171120 (2007).
24. D. P. Banks, K. S. Kaur, C. Grivas, C. Sones, P. Gangopadhyay, C. Ying, J. D. Mills, S. Mailis, I. Zergioti, R. Fardel, M. Nagel, T. Lippert, X. Xu, S. P. Banks, and R. W. Eason, "Femtosecond laser-induced forward transfer for the deposition of nanoscale, transparent, and solid-phase materials," *Proceedings of LAMP2009 - the 5th International Congress on Laser Advanced Materials Processing*, 1–9 (2009).
25. M. Duocastella, A. Patrascioiu, J. M. Fernández-Pradas, J. L. Morenza, and P. Serra, "Film-free laser forward printing of transparent and weakly absorbing liquids," *Opt. Express* **18**(21), 21815–21825 (2010).
26. A. Patrascioiu, J. M. Fernández-Pradas, J. L. Morenza, and P. Serra, "Microdroplet deposition through a film-free laser forward printing technique," *Appl. Surf. Sci.* **258**(23), 9412–9416 (2012).
27. R. Fernández, S. Bleda, S. Gallego, C. Neipp, A. Márquez, Y. Tomita, I. Pascual, and A. Beléndez, "Holographic waveguides in photopolymers," *Opt. Express* **27**(2), 827–840 (2019).
28. J. M. Liu, "Simple technique for measurements of pulsed Gaussian-beam spot sizes," *Opt. Lett.* **7**(5), 196–198 (1982).
29. Y. J. Liu and X. W. Sun, "Holographic polymer-dispersed liquid crystals: materials, formation, and applications," *Advances in OptoElectronics* **2008**, 52 (2008).
30. M. Ortuno, E. Fernandez, R. Fuentes, S. Gallego, I. Pascual, and A. Belendez, "Improving the performance of PVA/AA photopolymers for holographic recording," *Opt. Mater.* **35**(3), 668–673 (2013).
31. S. Gallego, D. Puerto, M. Morales-Vidal, M. G. Ramirez, S. I. Taleb, A. Hernández, M. Ortuño, and C. Neipp, "Tunable Waveguides Couplers Based on HPDLC for See-Through Applications," *Polymers* **13**(11), 1858 (2021).
32. A. Palla-Papavlu, V. Dinca, C. Luculescu, J. Shaw-Stewart, M. Nagel, T. Lippert, and M. Dinescu, "Laser induced forward transfer of soft materials," *J. Opt.* **12**(12), 124014 (2010).
33. F. Di Pietrantonio, M. Benetti, D. Cannatà, E. Verona, A. Palla-Papavlu, V. Dinca, M. Dinescu, T. Mattle, and T. Lippert, "Volatile toxic compound detection by surface acoustic wave sensor array coated with chemoselective polymers deposited by laser induced forward transfer: Application to sarin," *Sens. Actuators, B* **174**, 158–167 (2012).
34. C. B. Arnold, P. Serra, and A. Pique, "Laser Direct-Write Techniques for Printing of Complex Materials," *MRS Bull.* **32**(1), 23–31 (2007).
35. P. Delaporte and A.-P. Alloncle, "Laser-induced forward transfer: A high resolution additive manufacturing technology," *Opt. Laser Technol.* **78**, 33–41 (2016).
36. M. Duocastella, J. M. Fernández-Pradas, J. L. Morenza, and P. Serra, "Time-resolved imaging of the laser forward transfer of liquids," *J. Appl. Phys.* **106**(8), 084907 (2009).
37. C. W. Cheng, I. M. Lee, and J. S. Chen, "Femtosecond laser-induced nanoporous structures and simultaneous crystallization in amorphous indium-tin-oxide thin films," *Appl. Surf. Sci.* **316**, 9–14 (2014).
38. C. Lopez-Santos, D. Puerto, J. Siegel, M. Macias-Montero, C. Florian, J. Gil-Rostra, V. López-Flores, A. Borrás, A. R. González-Elipé, and J. Solís, "Anisotropic Resistivity Surfaces Produced in ITO Films by Laser-Induced Nanoscale Self-organization," *Adv. Opt. Mater.* **9**(2), 2001086 (2021).